Field-induced incommensurate spin structure of $TbNiAl_4$

W. D. Hutchison
School of Physical, Environmental and Mathematical Sciences, The University of New South Wales, Australian Defence Force Academy, Canberra, ACT 2600, Australia

D. J. Goossens* and R. E. Whitfield
Research School of Chemistry, Australian National University, Canberra, ACT 0200, Australia

A. J. Studer
Bragg Institute, Australian Nuclear Science and Technology Organisation, Lucas Heights NSW 2234, Australia

K. Nishimura and T. Mizushima
Graduate School of Science and Engineering, University of Toyama, Toyama 930-8555, Japan
(Received 8 November 2011; published 13 July 2012)

$TbNiAl_4$ exhibits incommensurate and commensurate magnetic ordering as a function of temperature. As a function of applied field it undergoes a series of magnetic phase transitions. The first of these transitions, into an intermediate spin arrangement, is the source of a large inverse magnetocaloric effect, an unusual result given that an aligning field is being applied. This has potential uses in magnetic cooling. Here, single-crystal neutron diffraction with applied magnetic field is used to obtain the intermediate field spin arrangement in $TbNiAl_4$. We find that not only does the applied field drive the system from commensurate to incommensurate ordering, but that the phase transition shows hysteresis such that a mixed state simultaneously showing commensurate and incommensurate antiferromagnetic ordering, along with ferromagnetism, can be obtained.

DOI: 10.1103/PhysRevB.86.014412 PACS number(s): 75.25.−j, 75.30.Kz, 75.30.Sg, 75.50.Ee

I. INTRODUCTION

The metamagnetic compound $TbNiAl_4$ has two magnetic phase transitions as a function of temperature and a previous neutron diffraction study established the nature of the three phases in the temperature manifold in zero applied field.[1] The three phases are (on cooling) paramagnetic, incommensurate (antiferro)magnetic, and linear antiferromagnetic [moments (anti)parallel to a]. The respective zero-field transition temperatures are 34.0 and 28.0 K, and propagation vectors for the two ordered phases are (i = incommensurate, c = commensurate) $\tau_i = (0.171\,1\,0.038)$ and $\tau_c = (0\,1\,0)$. Additionally, magnetization measurements show there are at least two phase transitions (three phases) as a function of magnetic field, applied along the easy a axis, at low temperatures.[2] Based on the observation of near full free ion Tb^{3+} moment, the highest field state (above 9 T at 4 K) is presumably a fully aligned (ferromagnetic) arrangement, while the low field state is a linear antiferromagnet. It is the unknown nature of the intermediate magnetic structure that is of interest here. Bulk magnetic measurements show an intermediate average (bulk) value for the Tb^{3+} moments in this phase, while low temperature nuclear orientation suggests that microscopically these moments remain high and essentially locally aligned (or antialigned) with the a axis above the transition.[3] That is, there is no sign of a spin flop as suggested by other authors.[2] There is additional interest in obtaining the intermediate field spin arrangement in $TbNiAl_4$ since it was recently shown that the field-driven magnetic phase transitions are the source of a large inverse magnetocaloric effect (ICME),[4] and as such field-controlled switching between phases may have applications in cooling at low temperatures. The implication is that the nature of the intermediate phase is important in the explanation of the ICME since it is the state that exists in the B,T range of interest.

II. EXPERIMENT: SINGLE-CRYSTAL NEUTRON DIFFRACTION

Single-crystal neutron diffraction as a function of magnetic field applied along the a axis was performed using the Wombat diffractometer at the OPAL reactor.[5] While Wombat is notionally a powder diffractometer, its two-dimensional, position-sensitive detector makes it a very powerful instrument for rapid acquisition of reciprocal space maps from single crystals—ideal for searching for potentially incommensurate magnetic Bragg reflections.

A $5 \times 5 \times 5$ mm^3 single crystal of $TbNiAl_4$ was mounted in a 7.4 T cryomagnet with the a axis vertical, as the magnet applies a vertical field. Neutron diffraction data were collected for sample angles, ω, varying through 145° in increments of 0.2°. The two-dimensional detector has an equator which spans 120°, and in this case the 2θ range was 15°–135°. The detector has a height of 200 mm, vertically centered at the incident beam and at a distance of ∼700 mm from the sample. This means that in single-crystal operation a scan of ω and 2θ maps out a volume of reciprocal space covering approximately ±8 degrees from the horizontal plane. $TbNiAl_4$ forms with the orthorhombic ($Cmcm$) structure, unit cells a, b, and c of 4.063(3), 15.415(6), and 6.603(4) Å, respectively.[6] Therefore with the bc plane in the equator of the instrument, and using a neutron wavelength of 2.41 Å, an experiment can measure out of the b^*c^* ($0kl$) plane as far as $h \sim 0.3a^*$. Given that from powder diffraction the a^* component of the incommensurate magnetic propagation

vector is thought to be $0.17a^* \sim 0.26$ Å^{-1},[1] reflections relating to incommensurate order can be noted simply by inspection of the three-dimensional (3D) reciprocal space map.

III. RESULTS AND DISCUSSION

The phase transitions with fields at low temperature can be seen in the magnetization data shown in Fig. 1. In particular, it can be noted that the Tb^{3+} moment in the highest field phase [$\sim 8.6\ \mu_B$ (Ref. 2] is close to what would be expected for ferromagnetically aligned free ion moments ($9.0\ \mu_B$). The intermediate phase shows a much reduced average (bulk) magnetic moment compared to either the staggered antiferromagnetic moment in zero field[1] or to the high-field moment; however, there is significant field hysteresis associated with the lower transition as might be expected for a ferromagnetic system.

Figure 2 contains 3D plots of zero-field data corresponding to the experimental conditions (b) and (c) of Table I, respectively. They illustrate the volume of reciprocal space accessed by the experiment and show the stark contrast in the location of the commensurate (indicated by darker colored spots) and incommensurate (lighter) magnetic reflections. The plot shows the plane normal to a (or a^*), passing through the origin. [A point in this reciprocal plane will have coordinates (q_a,q_b,q_c) with $q_a = 0$ or alternatively hkl where $h = 0$). This b^*c^* plane, indicated by the darkened disks in Fig. 2, contains a strong series of Bragg reflections including both structural and, at low temperature, commensurate magnetic intensities. In contrast, the incommensurate magnetic phase(s) exhibit a series of diffracted intensities above and below the plane at $h \sim \pm 0.17$ [Fig. 2(b)].

To further illustrate what is shown by these diffraction data, it is convenient to examine 2D slices of reciprocal space in which both commensurate and incommensurate spots are apparent. Since the c^* component of the incommensurate propagation vector is very close to zero,[1] slices normal to c^* with l an integer, for example the $hk1$, can be used. Such slices of reciprocal space measured for the range of different conditions are shown in Fig. 3. The vertical coordinate is h (or

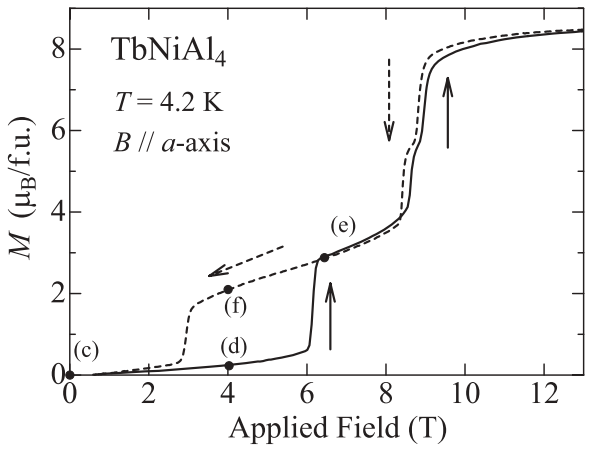

FIG. 1. Magnetization curve for $TbNiAl_4$ with the magnetic field applied parallel to the a axis at 4.2 K. The arrows show the increasing- and decreasing-field magnetization curves. The letters and black dots indicate points at which diffraction data were collected (see Table I).

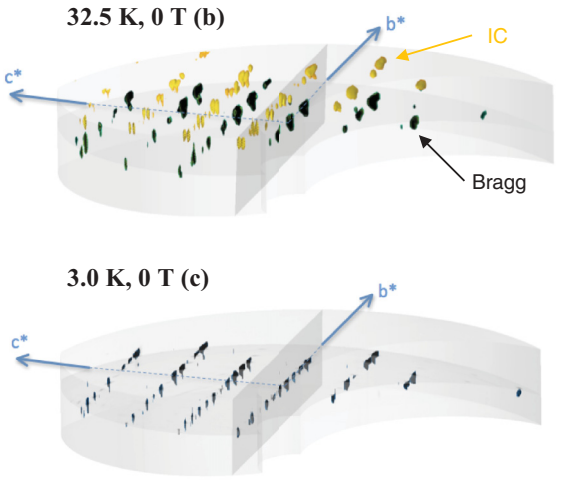

FIG. 2. (Color online) 3D representations of the region of reciprocal space viewed in these experiments. The darkened horizontal disks, which contain the b^* and c^* directions, indicate the b^*c^* plane. The vertical slices are at $l = 1$ as used in Fig. 3. The upper figure, a measurement at 32.5 K and zero field, has structural Bragg intensities (darker spots) in the b^*c^* plane and incommensurate magnetic reflections (lighter spots) above and below (not shown) this plane. Example reflections, one of each type, are labeled Bragg and IC, respectively. The lower figure, a result at low temperature (3.0 K) and zero field, has both structural and commensurate magnetic reflections which are all in the b^*c^* plane. Letter labeling matches Table I.

q_a if preferred) and the horizontal coordinate is k; $l = 1$ in this section. The vertical dimension is exaggerated.

Figure 3(a) shows the scattering at 60 K (zero field), above all the magnetic phase transition temperatures, in the paramagnetic phase. The Bragg intensity comes from nuclear (structural) neutron diffraction only, with the 081 peak noted. The arrowed peak is an example of scattering from a small second crystal incorporated into the sample; peaks from this crystal behave like those of the larger crystallite, and can usually be factored out.

Figure 3(b) shows the same region of reciprocal space measured at 32.5 K. Arrowed are two of the many incommensurate magnetic diffraction peaks corresponding to $\tau_i \sim (0.171\ 1\ 0.04)$; they are stronger above the $h = 0$ row of peaks than below because of asymmetrical sample shielding.

Figure 3(c) gives the same region at lower temperature ($T = 3.0$ K) and zero field; the incommensurate magnetic peaks have vanished and commensurate magnetic peaks appear

TABLE I. Conditions under which diffraction data were collected. Labeling corresponds to that used in the figures.

Label	Temperature (K)	Applied field (T)
(a)	60.0(3)	0
(b)	32.5(3)	0
(c)	3.0(3)	0
(d)	3.5(3)	4
(e)	3.5(3)	6.3
(f)	3.5(3)	4

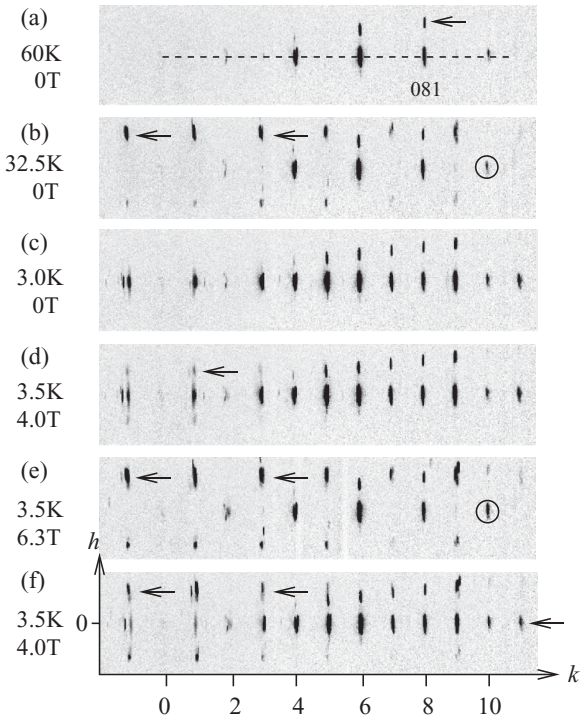

FIG. 3. Reciprocal space maps of the $hk1$ section under different conditions of field and temperature. Labeling matches that of Table I and Fig. 1. Black denotes high intensity and white denotes low intensity; key features have been arrowed.

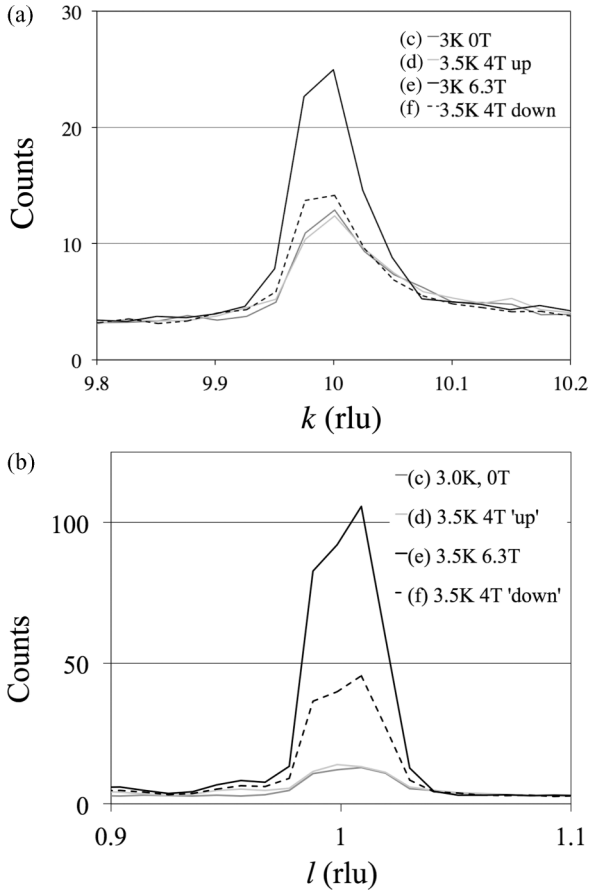

FIG. 4. (a) A comparison of the reflected neutron intensity cutting through the (0 10 1) nuclear reflection in the $\hat{k}$ direction, showing the ferromagnetic Bragg peak induced at high field. Intensities have been averaged over a band 20 pixels wide around the direction indicated by the dashed line in Fig. 3(a). (b) Shows the same result cutting through the (0 2 1) nuclear Bragg peak in the $\hat{l}$ direction.

at odd values of k [note that there is no evidence in (b) for intensity at these points], where the nuclear structure only gives intensity for even k.

For Fig. 3(d), $T = 3.5$ K and a magnetic field of 4 T was applied along the a axis. It can be seen that the commensurate magnetic ordering is maintained, although there are some weak peaks above and below the lower-order reflections (an example is arrowed), possibly indicative of some continuous evolution of the incommensurate component. As the field continues to increase, and T remains low, the ordering is driven into the incommensurate state. The incommensurate peaks arrowed in (e) are within error of the same positions as those in (b) [$\tau_i \sim (0.171\ 1\ 0.04)$]. However, there are significant differences—some "nuclear" peaks show increased intensity. This is particularly evident for (0 2 1) and (0 10 1) [the latter is circled in (b) and (e) and both are shown in detail in Fig. 4], and implies the presence of a ferromagnetic component. This is not apparent in comparing (d) with (c), and it appears that the ferromagnetic component is only strong at this highest field, and as Fig. 4(b) shows, some of this ferromagnetic intensity is maintained on returning to 4 T (f), in accordance with the magnetization data shown in Fig. 1. Also, on reducing the field back to 4 T (f), *both* the commensurate and incommensurate magnetic reflections are present. On further reduction of field to 0 T, the system returns to the commensurate-only ordering as apparent in (c).

The evolution of the commensurate magnetic peaks as field is increased and then decreased is shown in Fig. 5. Quite clearly the intensities of the nuclear peaks ($k = 2n$) are relatively constant, while the commensurate magnetic intensity is much lower for case (f), which is after the sample has been subjected to high fields. Data from collection (e) is not shown here because there is no commensurate magnetic intensity. For all magnetic peaks, the reduction in intensity is very similar—the integrated intensity of magnetic peaks for data set (f) is $\sim$50% of that for (c) or (d). This suggests that rather than the commensurate moment changing direction, a large fraction of the sample has not returned to the commensurate state on returning to 4 T. In data set (d), the magnetic intensity is within error the same as in (c) for peaks with both $l \gg k$ and $k \ll l$; this indicates that the system is not going through a spin flop transition as field is increased, as was suggested by Ref. 2, but rather the behavior is in accordance with the low temperature nuclear orientation result of Ref. 3 whereby the Tb^{3+} moments were found to remain aligned, or antialigned, during a field sweep.

The incommensurate intensity is larger when induced by field rather than temperature, with the incommensurate peaks for (e) (3.5 K, 6.3 T) being approximately double the size of those in (b) (32.5 K, 0 T). This can largely be explained through the Brillouin function for the moments. For (f), where the commensurate phase is also present, the positions of the incommensurate peaks remain unchanged relative to (b) and

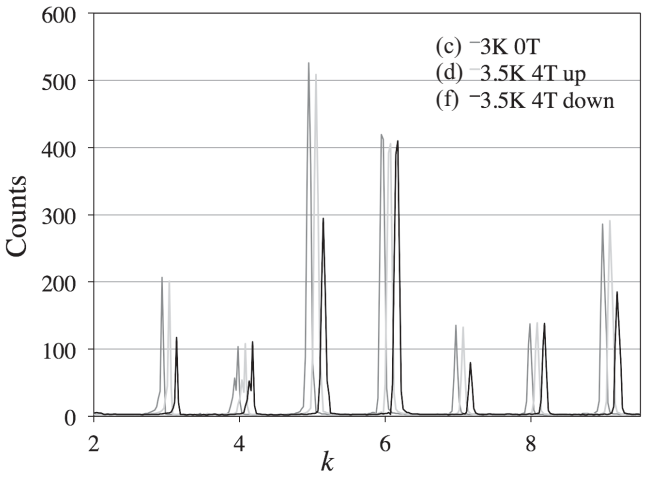

FIG. 5. A comparison of the reflected neutron intensity in commensurate magnetic Bragg peaks, as a function of position in reciprocal space along $(0\,k\,1)$. Data sets (d) and (f) are offset horizontally for easier comparison. "up" indicates that the magnetic field is increasing from zero, and "down" indicates that the field has been reduced from its maximum before the measurement was made. Purely magnetic reflections occur at $k = 2n + 1$; other peaks are from nuclear scattering. Intensities have been averaged over a band 20 pixels wide around the direction indicated by the dashed line in Fig. 3(a).

(e), but the intensities are lower than in either (b) or (e), supporting the conclusion that the sample has entered a mixed phase with only a fraction of the sample in the incommensurate state. A number of the incommensurate peaks overlap with the commensurate peaks for the second crystallite, but comparison of the peaks arrowed in (b) and (e) with their equivalents in (f) shows that at least $\sim$20% of the sample is in the incommensurate state.

Correlation of the results above with measurements of the entropy of the materials show that the IMCE occurs when the system is in the incommensurate magnetic state.[4] However, unlike many MCE materials[7,8] there is no structural transition associated with the change in entropy—it is entirely magnetic in origin. Further, $TbNiAl_4$ is a fully stoichiometric material, unlike, for example, the manganite oxides such as $Pr_{0.46}Sr_{0.54}MnO_3$.[9] The Ni shows no magnetic ordering, and so the MCE effects can be solely ascribed to the ordering of the Tb moments. Further, it is generally considered that "inverse MCE is observed in systems where first-order magnetic transformations, such as antiferromagnetic/ferromagnetic (AF/FM), AF-collinear/AF-noncollinear or antiferromagnetic/ferrimagnetic (AF/FI), take place".[10] Broadly, the $TbNiAl_4$ case fits this definition in that it has a transition from AF collinear to an incommensurate state that can be described as AF with a ferromagnetic moment, i.e., macroscopically like a ferrimagnet.

The basic requirement to obtain IMCE is that the sample cools down when the field is applied, meaning that $\Delta S > 0$ and $\Delta T < 0$ and the temperature derivative of the magnetization is positive; this has been very comprehensively discussed.[11] However, for a single-crystal system such as $TbNiAl_4$ where the magnetic field is being applied along the a direction, the parallel antiferromagnetic susceptibility $\chi_{||}$ will be observed, which is of very small magnitude for low T. Upon applying the field, and obtaining the incommensurate (IC) phase through a first-order transition, the system goes into a state which is still broadly described as AF with the moments remaining parallel to a, but in a superlattice configuration, and with on average more of the moment aligned than antialigned with the field. Furthermore the amount of aligned moment in this IC phase increases with increasing temperature, at constant field,[4] adding to the IMCE. Interestingly, this does not require the introduction of substantial field-induced disorder, although disorder has been mentioned as a key aspect of the phenomenon for some materials.[11]

There is no reason to suppose the existence of a disordered component of the magnetic moment in the field-induced incommensurate state. Certainly there is no measurable increase in background with increasing field, even comparing 3 K, 0 T to 3.5 K, 6.3 T [data set (c) to data set (e)]—the disorder of large magnetic moments such as those found on the Tb would give rise to significant unstructured scattering, distributed according to the magnetic form factor of the Tb^{3+} ion, something that *is* apparent as the temperature increases.[1] Further, comparison of the incommensurate peaks induced by temperature [data set (b)] and field [data set (e)] shows that the incommensurate order induced by field has, to within error, the same propagation vector as that induced by temperature, but the magnitude of the moments is much greater (Fig. 6), again suggesting that there is little moment lost to disorder. Therefore we conclude that $TbNiAl_4$ has a single incommensurate phase spanning the intermediate region of B,T space as illustrated in the phase diagram of Fig. 7. Throughout this phase the IC propagation vector, and therefore the AF periodicity, is fixed but the magnitude of the net ferromagnetic moment, based on the relative combined strength of the average parallel and antiparallel moments, varies with applied field and temperature. The mixed phase region (AF + IC), noted above and accessed (hysteresis-like) only via downward field sweeps is also indicated in Fig. 7.

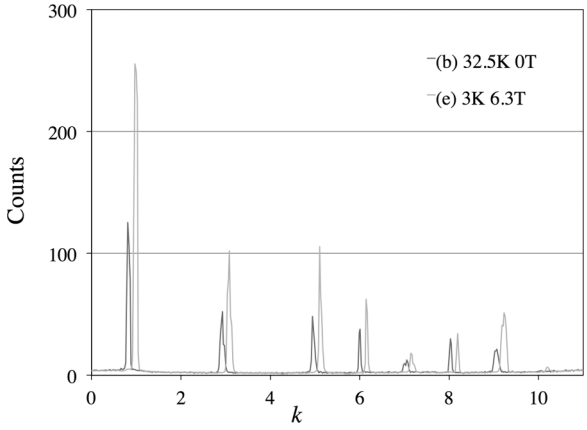

FIG. 6. A comparison of the reflected neutron intensity in incommensurate magnetic Bragg peaks, as a function of position in reciprocal space along $(0.17\,k\,1)$. Data sets (b) and (e) are offset horizontally for easier comparison. Purely magnetic reflections occur at $k = 2n + 1$; the small peaks at $k = 2n$ are due to the second crystallite. Intensities have been averaged over a band 20 pixels wide.

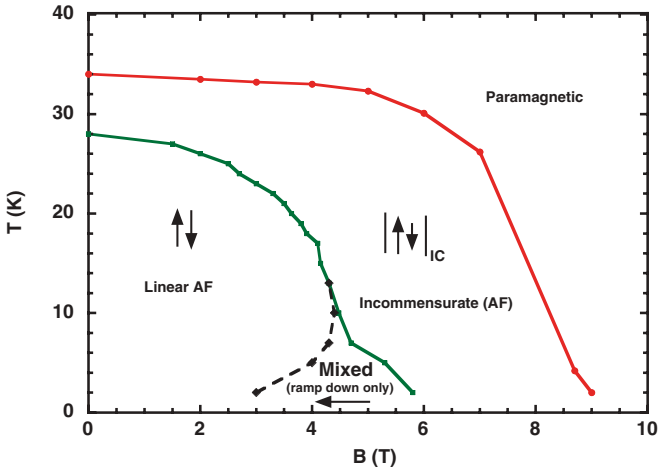

FIG. 7. (Color online) Phase diagram for $TbNiAl_4$ based on the knowledge of magnetic structures from this work and Ref. 1, as well as transition fields and temperatures derived from the magnetization and specific-heat measurements of Refs. 1, 2, and 4. There are three main magnetic structure regions: linear AF, incommensurate AF (IC) within which there is a variable ferromagnetic component, and paramagnetic. In addition, as identified in this work, there is a mixed phase region (AF + IC) which is only created via a hysteretic cycling of the field at low temperatures.

IV. CONCLUSIONS

The negative magnetocaloric effect in $TbNiAl_4$ is due to a field-induced magnetic phase transition from a commensurate antiferromagnetic low-field state to an incommensurate magnetic structure with ferromagnetic component and the subsequent increase in this net moment as the IC region is traversed. The incommensurate propagation vector of the field-induced phase is within error of being the same as the that of the incommensurate phase induced by an increase in temperature, leading to the conclusion that there is just one incommensurate phase but with a variable net ferromagnetic component. This ferromagnetic component is not indicative of a conventional metamagnetic transition;[4] rather it should be thought of as a "dc" shift of the antiferromagnetically correlated spin components.

All of the magnetic behavior within $TbNiAl_4$ is due solely to the Tb^{3+} moments. The incommensurate magnetic phase can be described essentially as commensurate planes of these spins with an incommensurate modulation in the perpendicular direction (*a* axis). The conditions for magnetic order, including the IC phase, and the criticality for phase transitions are determined by the interplay between Tb^{3+} exchange and crystal field anisotropy, with an applied magnetic field modifying the equilibrium. This is a scenario that is commonplace in rare-earth-based systems, even though the IC state itself is somewhat unusual. There is a strong contrast, however, with other classic classes of materials that show field-driven transitions to incommensurate phases such as systems involving spin chains and lattice deformation,[12] or AF spin flops,[13] where the IC phase can only exist in applied fields, or spiral magnets that can be driven incommensurate solely by the applied magnetic field.[14]

Ferromagnetic hysteresis is apparent in the diffraction experiments; it is found that on increasing the magnetic field from 0 T the incommensurate phase is not seen at 4 T, but is seen at 6.3 T up to at least 7.4 T, while on reducing the field back to 4 T from 7.4 T, the incommensurate phase persists and the sample falls into a mixed magnetic state, with approximately 50% of the sample showing commensurate magnetism at 3.5 K, 4 T. This is in accord with the temperature-induced behavior[1] which suggests a first-order transition from the commensurate to incommensurate phase, consistent with a system that can be driven into a mixed state.

Further, the ICME does not seem to rest on magnetic disorder, but on a first-order transition from a collinear AF to incommensurate magnetic state, the latter having a variable net moment which increases with an increase in temperature within this phase region. Neither state shows evidence for magnetic disorder.

ACKNOWLEDGMENTS

We gratefully acknowledge the Bragg Institute for a grant of beam time and the Australian Research Council and the Australian Institute of Nuclear Science and Engineering for financial support. D.J.G. acknowledges the support of the Australian Research Council.

*goossens@rsc.anu.edu.au

[1] W. D. Hutchison, D. J. Goossens, K. Nishimura, K. Mori, Y. Isikawa, and A. J. Studer, J. Magn. Magn. Mater. **301**, 352 (2006).
[2] T. Mizushima, Y. Isikawa, A. Mitsuda, K. Kobayasi, F. Ishikawa, T. Goto, and S. Kawano, J. Magn. Magn. Mater. **272–276**, E475 (2004).
[3] W. D. Hutchison, L. K. Alexander, and K. Nishimura, Hyperfine Interact. **197**, 111 (2010).
[4] L. Li, K. Nishimura, and W. D. Hutchison, Solid State Commun. **149**, 932 (2009).
[5] A. J. Studer, M. E. Hagen, and T. J. Noakes, Physica B: Condensed Matter **385–386**, 1013 (2006).
[6] P. Villars, *Pearson's Handbook Desk Edition* (ASM International, Pearson's Handbook, Materials Park, OH, 1997).
[7] V. K. Pecharsky and K. A. Gschneidner, Appl. Phys. Lett. **70**, 3299 (1997).
[8] V. K. Sharma, M. K. Chattopadhyay, and S. B. Roy, J. Phys. D **40**, 1869 (2007).
[9] V. B. Naik, S. K. Barik, R. Mahendiran, and B. Raveau, Appl. Phys. Lett. **98**, 112506 (2011).
[10] T. Krenke, E. Duman, M. Acet, E. F. Wassermann, X. Moya, L. Manosa, and A. Planes, Nature Mater. **4**, 450 (2005).
[11] P. J. von Ranke, N. A. de Oliveira, B. P. Alho, E. J. R. Plaza, V. S. R. de Sousa, L. Caron, and M. S. Reis, J. Phys.: Condens. Matter **21**, 056004 (2009).
[12] V. Kiryukhin, B. Keimer, and D. E. Moncton, Phys. Rev. Lett. **74**, 1669 (1995).
[13] D. C. Dender, P. R. Hammar, D. H. Reich, C. Broholm, and G. Aeppli, Phys. Rev. Lett. **79**, 1750 (1997).
[14] I. E. Dzyaloshinskii, Sov. Phys. JETP **20**, 665 (1965).